A. Specific Aims

This funded proposal has two specific aims:

Aim 1: Measure the nephron endowment and distribution of glomerular volumes in the healthy and nephrotic human kidney with MRI.

Aim 2: Develop a robust, <u>automated</u> image segmentation algorithm and software to measure whole kidney nephron endowment, glomerular volume, and glomerular permeability in the kidney.

B. Studies and Results

We have completed the baseline work for Aims 1 and 2, having completed a full study under this grant of 10 human kidneys. Our progress toward the Aims of this grant and the significance of our work in light of our most recent studies is described below, and published in our recent papers (1-3), two conference proceedings (4-5) and a paper in submission (6).

We focused most of our efforts in this goal on establishing our ability to detect and measure the number and volume of glomeruli in the intact human kidney.

B.1. Pilot study in four human donor kidneys and one control

To investigate the use of CF as a glomerulus-specific MRI contrast agent in humans, cationic ferritin (CF) was injected into the renal artery of three viable (but un-transplantable) human donor kidneys within 24 hours of resection. Saline was injected into one kidney instead of CF as a control. The CF-injected kidneys are hereafter referred to as kidney CF1, CF2, and CF3. The donors had diverse backgrounds, various causes of death, and large variations in kidney function. The donor data were investigated to establish possible reasons for any variability in nephron number and CF accumulation in the kidneys measured by MRI (see *Pathology* section). These data are shown in Table 1. Notably, the donor of kidney CF2 suffered from severe, untreated hypertension, and the donor of kidney CF1 suffered from mild, treated hypertension.

MRI (Aim 1)

We imaged the intact, fixed donor kidneys on a 7T MRI scanner using a 3D gradient-recalled echo pulse sequence (resolution = 117x117x117 μm^3). As shown in Fig. 1A, the MR images exhibited dark spots throughout the renal cortex of the CF-injected kidneys. Each dark spot in the cortex corresponds to a single glomerulus and is ~50-80% darker than the surrounding cortex. These dark spots were not present in the un-injected control kidney (Fig. 1D). The punctate spots of glomeruli in images of the CF-injected kidneys were caused by the accumulation of the superparamagnetic CF to the GBM. The labeled glomeruli defined the boundary between the
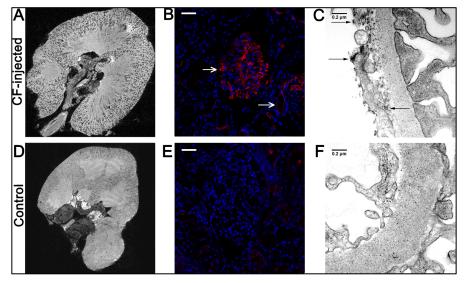

Figure 1: Intravenously injected CF specifically labels glomeruli in perfused human donor kidneys, making them visible with 7T MRI. MRI of CF-labeled human kidneys reveals punctate dark spots throughout the cortex, with each spot associated with a single glomerulus (A). A naive control kidney showed minimal signal loss caused by residual blood (D). Immunofluorescence confirmed the accumulation of CF (red) in glomeruli and leakage of CF into tubules of CF inoculated kidneys (B). Naive control glomeruli remained clear of CF-related immunofluorescence (E). Transmission electron microscopy (TEM) confirmed the accumulation of CF to the glomerular basement membrane and the endothelial glycocalyx (C). The glomerular capillary walls of the naive control kidney were clear of any punctate TEM signal darkening associated with the accumulation of CF (F). White scale bars = 50 μm. Black scale bars = 200 nm.

cortex and the medulla and revealed the individual lobes and papillae of the kidney. The specific binding of CF to the glomerulus and tubule was confirmed with immunofluorescence microscopy (Fig. 1B and E). Transmission electron microscopy also showed the CF bound to the GBM and to endothelial surfaces of the glomerular capillary wall (Fig. 1C and F).

To assess the possibility of detecting glomeruli in a typical clinical MRI, a CF-labeled kidney was imaged at low resolution on a clinical 3T MRI scanner. While individual glomeruli were not visible with the lower image resolutions achieved with this MRI system ($270 \times 270 \times 540$ μm^3), the average signal magnitude in the cortex of the CF-labeled kidney was ~20% lower than its medulla. Minimal differences were seen in signal magnitude between the cortex and medulla (<2%) in the control kidney. Thus, gross CF ccumulation was detected in the kidney using a typical 3T MRI by measuring the ratio of cortical to medullary image intensity (data not shown).

Leakage of CF through the GBM into the proximal tubule was vivible MRI images of kidneys CF1 and CF2 (Fig. 2A, Fig. 2A and D, and zoomed panels of Fig. 5), and was also visible in immunofluorescence microscopy (Fig. 1B). This leakage was similar in appearance to leakage observed in a rat model of focal and segmental glomerulosclerosis[15]. MR image darkening associated with glomerular labeling in the hypertensive kidney CF2 was diffuse in many regions, likely due to leakage of CF through the glomerulus into the proximal tubule. Large regions of the cortex of this kidney also lacked labeled glomeruli in MRI. Histopathological analysis (detailed below) suggested this was due to severe glomerular and arteriole sclerosis that prevented perfusion of those areas. Importantly, the serum creatinine in this patient was only slightly elevated, even with gross kidney pathology.

Pathology

A histopathological analysis was performed on each kidney by a renal pathologist using light microscopy. Histopathology of kidney CF1 revealed four sclerotic glomeruli of the 72 examined. There was widespread patchy fibrosis and tubular dilation and
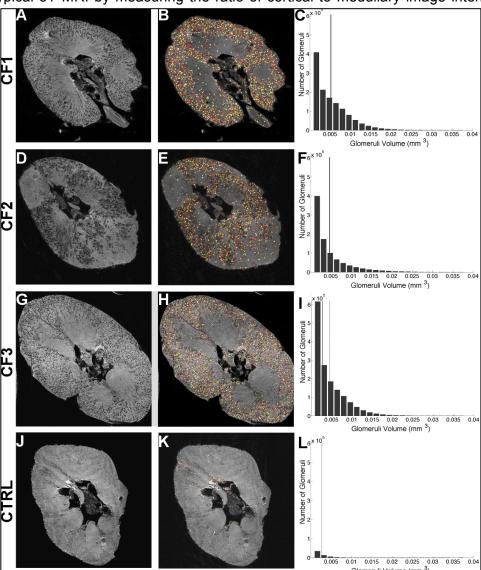

Figure 2: Glomeruli are visible in 7T MRI in all three CF-inoculated kidneys (A, D, and G). An automated image segmentation algorithm was able to identify labeled glomeruli (B, E, and H). Identified glomeruli are assigned an arbitrary color for the purpose of visualization. The control (un-inoculated) kidney shows very few regions defined as 'glomeruli' - most of which are likely attributed to residual blood. The MRI-measured apparent intra-renal glomerular volume distribution for each kidney are shown along with a grey line showing the mean MRI-measured aVglom and a black line showing the measured Vglom using stereology (C, F, I, and L). Note that the grey and black lines overlap in panel F, and that no stereology measurement was made of the control kidney.

atrophy with mild diffuse lymphohistiocytic leukocytic infiltration within the interstitium. The arteries were sclero tic with variable hyalinosis. Overall there was minor nephrosclerosis and acute tubular injury.

Histopathology of a random section of kidney CF 2 revealed five totally sclerosed glomeruli of the 61 examined and one with perihilar segmental sclerosis. Because of the patchy nature of CF-labeling in this kidney (revealed by MRI), we separately examined tissue sections from the labeled and unlabeled regions in detail. In the regions of CF-labeled tissue, the interstitium had widespread mild, patchy fibrosis. The tubules were mildly dilated and atrop

hic, and a moderate lymphohistiocytic infiltrate was present that included eosinophils. The arterioles were tortuous and showed marked hyalinosis with endothelial sclerosis. Within the unlabeled regions, the degree and number of severely sclerotic glomeruli was striking. Vascular involvement was evident, with both the arteries and arterioles severely thickened. In some unlabeled areas, it was impossible to distinguish sclerotic glomeruli from obstructed arterioles. The tubules in the unlabeled areas were unaffected overall, but did occasionally contain cast material. Overall, kidney CF2 had moderate nephrosclerosis, with vascular evidence of significant hypertensive damage. We concluded that the observed lack of CF-labeled glomeruli in kidney CF2 was correlated with focal sclerosis and vascular damage at those locations.

Histopathology of kidney CF3 revealed one sclerotic glomerulus of the 66 glomeruli examined, with no mesangial proliferation or segmental sclerosis within the glomeruli. The interstitium showed slight fibrosis and tubular atrophy with minimal lymphohistiocytic interstitial inflammatory infiltrate. The arteries were either normal or had mild sclerosis of the intima. The tubules were mildly dilated with scattered uromodulin casts. Overall, there were only very mild changes of acute tubular injury and very mild background nephrosclerosis.

Quantitative Morphology (Aim 2)

We developed and applied custom software to measure glomerular number and individual glomerular volume from the MR images. The custom 3D image processing software identified and measured labeled glomeruli in the MRI volumes of CF-inoculated kidneys (Fig. 2B, E, H, and K). In the panels, identified glomeruli are assigned an arbitrary color to
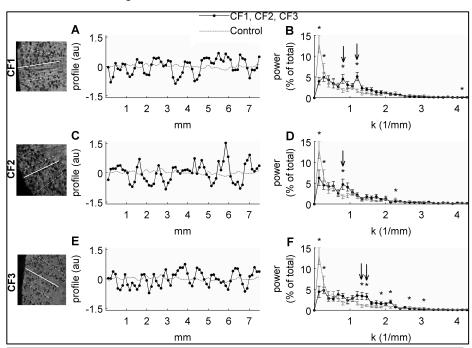

Figure 3: Line profiles (16 per kidney) were drawn through the cortex of each kidney. Here the line signal profiles of the solid white line profiles are plotted (A, C, and E) and the mean power spectrum for the 16 line profiles are shown (B, D, and F). Black traces are data from CF-inoculated kidneys and grey traces are data from the naive control. Arrows point to spatial spectral peaks of particular interest. Qualitatively, the line profiles drawn in each kidney appear different from one another, with the the CF1 line profiles being composed of a superposition of high and low frequency components, the CF2 line profile being mostly composed of relatively low frequency oscillations, and the CF3 line profiles being mostly composed of relatively high frequency oscillations. The line profile signal changes associated with the appearance and disappearance of sites of CF-accumulation in the CF1 kidney correspond to two spectral peaks; one at $k = 0.8$ mm^{-1} (4.5% of total signal) and one at $k = 1.2$ mm^{-1} (5% of total signal). The line profile signal changes associated with the accumulation of CF in the CF3 kidney correspond only to high frequency spatial oscillations between $k = 1.2$ and 1.5 mm^{-1} which account for 10% of the total signal along the line profiles. Stars represent a statistically significant difference between the CF-inoculated kidney and the naive control ($\alpha = 0.04$) and arrows denote peaks of particular interest. Error bars represent mean ± one standard deviation between power spectra of sixteen randomly chosen line profiles.

visually distinguish them from neighboring glomeruli. We next compared the results of the MRI-based measurements to those obtained through disector/fractionator stereology on the same kidneys. The number of glomeruli identified by the software yielded the total apparent number of glomeruli per kidney (aNglom) of 1.27×10^6, 0.92×10^6, and 1.52×10^6 glomeruli, compared to stereological counts of 1.13×10^6, 0.74×10^6, and 1.46×10^6, for CF1, CF2, and CF3 kidneys, respectively. Both MRI- and ster

Stereology-based measurements were consistent with the range of Nglom reported in the literature[24]. The software counted 0.057×10^6 false glomeruli in one naive control kidney, yielding a false-positive rate of the image processing algorithm of ~6%.

Using the same software, we measured the glomerular volumes based on the number of voxels in each glomerulus in the 3D MR images. The median MRI-based apparent glomerular volumes (aVglom) were 4.8×10^{-3} mm^3, 3.2×10^{-3} mm^3, and 3.2×10^{-3} mm^3 for CF1, CF2, and CF3, respectively. Stereology median Vglom estimates were 5.01×10^{-3} mm^3, 4.68×10^{-3} mm^3, and 2.82×10^{-3} mm^3. These volumes are consistent with those reported in the literature[24]. The MRI-based measurements were also used to generate histograms of the distribution of glomerular volumes within each kidney. These distributions cannot be detected with other current techniques. Histograms of the intra-renal aVglom distribution for each labeled kidney are shown in panels C, F, I, and L of Figure 2. Skewness of the distribution was 1.5, 2.2, and 1.7 for CF1, CF2, and CF3, respectively, representing the tendency of the distributions to deviate from the mean.

Image texture analysis

We performed image texture analysis to detect morphological differences between MRI volumes of CF-labeled donor kidneys (Fig. 3), consisting of the spatial power spectrum associated with line profiles randomly drawn in the cortex in the MR images.

The line profile image oscillations associated with the appearance and disappearance of sites of CF-accumulation in the CF1 kidney, which showed only mild nephrosclerosis in histopathology, appeared to be a mix of high and low spatial frequencies. The average power spectrum from the CF1 kidney revealed two CF-related spatial spectral peaks; one at k = 0.8 mm^{-1} (4.5% of total signal power) and at k = 1.2 mm^{-1} (5% of total signal power).
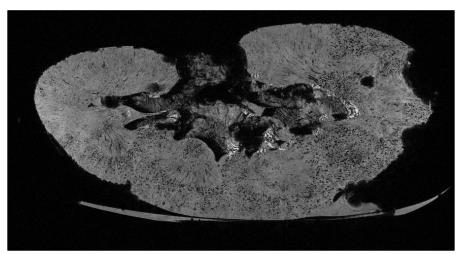

Figure 4: 3D GRE-MRI of a human kidney after intravenous CF injection. CF-labeled glomeruli are visible surrounded by large regions with no labeling, similar to what we observed in hypertensive, sclerotic patients.

The image magnitude profiles in kidney CF2, histopathologically assessed as the least healthy kidney of the group, had a relatively low frequency CF-related oscillation compared to the healthier CF3 kidney. The average power spectrum from the CF2 kidney revealed a CF-related spatial signal oscillation at k = 0.8 mm^{-1} which accounted for 5% of the total signal power along the line profiles.

The line signal profiles in CF3, defined by histopathology as the healthiest kidney of the group (discussed below), demonstrated high spatial frequency oscillations between k = 1.2 and 1.5 mm^{-1} and account for 10% of the total signal power along the line profiles.

B.2. Extension to diabetic population (Aims 1 and 2)

To date we have received four human kidneys from diabetic donors. We have performed MRI as described above. A representative image of one of these kidneys (confirmed diabetic nephropathy) is shown in Figure 4. We are currently analyzing the histology of these kidneys to determine whether there is reduced perfusion due to sclerotic vasculature or glomerular hypertrophy. However, these data are strongly suggestive of the potential for this technique in the early detection of kidney disease and in transplant characterization.

C. Significance

The ability to measure changes in glomerular morphology and local protein leakage in the clinic has the potential to directly improve patient care and clinical outcomes. A technique to assess glomerular morphology and protein leakage could be used to assess the viability of kidneys from both living and deceased donors, ensuring that a donor kidney has sufficient filtration surface area.. It would also allow younger recipients to receive kidneys with a nephron number sufficient to match their lifespan.. Furthermore, individuals at risk for chronic kidney disease, such as those who have had acute kidney injury, nephrotoxins, premature birth, hypertension, or diabetes, could receive an individualized risk assessment using this technique. Early detection and regular monitoring of kidney disease would enable early education and therapy to halt disease progression. Finally, *In vivo* use of CF and MRI to monitor kidney health in drug trials could allow subjects to be taken off experimental drugs before substantial damage has occurred.

A long term goal of this work is to improve clinical outcomes using MRI as a tool to diagnose and monitor the progression of kidney diseases in patients. Studies of the toxicity and bio-distribution of CF, the development of new, highly-sensitive, glomerulus-specific MRI contrast agents, and advancements in RF hardware for high resolution *in vivo* MRI of the kidney[18] are in progress. Production of recombinant human ferritin may further reduce toxicity. Finally, substantial work must be done to accurately apply the glomerular measurement algorithm in diseased kidneys.

D. Plan

We have made significant progress toward the Aims of the proposal over the past year of funding. We will continue to analyze our collected data, building a database of MRI-detected morpohology in the human kidney in patients. We are coupling our experimental efforts with a focus on large-scale data analysis to identify potential early markers of human kidney and cardiovascular disease.

E. Publications

1. J. Charlton, S.C. Beeman, and **K.M. Bennett***, MRI-detectable nanoparticles: The potential role in the diagnosis of and therapy for chronic kidney disease. *Adv Chron Kid Disease. 2013*. 20(6):479-87.2. K.M. Bennett, S.C. Beeman, J. Bertram, N. Gretz.

2. **K.M. Bennett***, S.C. Beeman, J. Bertram, N. Gretz. The emerging role of MRI in quantitative renal glomerular morphology. *Am J Physiol Renal Physiol*. 2013. 304(10):F1252-7.

3. J.F. Bertram*, L.A. Cullen-McEwen, G. Egan, N. Gretz, E. Baldelomar, S.C. Beeman, and **K.M. Bennett**. How and why we measure nephron number. *Pediatric Neprology 2013* (In Press).

4. S.C. Beeman, E.J. Baldelomar, J.F. Bertam, J.R. Charlton, and K.M. Bennett. Counting glomeruli in a human transplant kidney using MRI. Proc Int Soc Magn Reson Med, Salt Lake City, UT. 2013.

5. S.C. Beeman, J.F. Bertram, M. Zhang, T. Wu, J.R. Charlton, **K.M. Bennett**. MRI detectable nanoparticles to measure the size and number of glomeruli in the human kidney. American Society for Nephrology, 2013, Atlanta, GA. USA.

6. S.C. Beeman, J. Bertram, **K.M. Bennett***. MRI measurements of nephron endowment and glomerular volume in human kidneys. *JASN* (In submission).